POST-BUCKLED BEHAVIOUR INVESTIGATION USING A NONLINEAR FINITE ELEMENT ANALYSIS

ICAS-94-9.8.4

A.J. TANNER

BRITISH AEROSPACE AIRBUS LTD.

ABSTRACT

This paper demonstrates the use of a nonlinear finite element analysis technique for the investigation of combined shear and compression post-buckled behaviour of a typical wing spar structure as designed and manufactured by British Aerospace Airbus Ltd. An experimental test programme was conducted on a full size section of wing spar with a limited representation of wing skin/stringer structure. The test structure was analysed using NIKE3D, an implicit nonlinear finite element code, developed by Lawrence Livermore National Laboratory. Material plasticity and geometric nonlinear effects resulting from both combined compression and shear buckling of the spar were included. The analysis was used to predict stresses, strains and displacements during loading, and also to assess the failure mode of the spar specimen. In particular the post-buckled behaviour of the structure was investigated. Generally good agreement was obtained between the analysis and experimental results.

INTRODUCTION

Modern commercial transport aircraft design philosophy has been influenced by the need to provide an economically competitive aircraft whilst improving its overall safety. This has placed increased demands upon designers to improve the overall structural efficiencies of the aircraft primary structure. The design of Airbus wing box structures makes extensive use of integrally machined structural components. In particular the wing box spars are machined from aluminium alloy rolled plate. By using this manufacturing method wing box structures compliant with overall aerodynamic and strength requirements may be obtained at reasonable cost.

The concurrent engineering approach to structural design, combined with the need to exploit improvements in structural efficiency, requires an early and comprehensive understanding of a structure's behaviour up to ultimate failure, prior to the commitment of large manufacturing costs. This places far greater demands upon structural analysis techniques in order to reduce the cost of development programmes.

Conventional analysis techniques are available to assess the strength and buckling characteristics of these spar structures. However, with these techniques it is difficult to perform detail investigations to include the interaction between shear and compression buckling effects, plasticity, and the changes in spar geometry, which take place before ultimate failure. Nonlinear finite element methods have the potential to address all of these areas, and in addition investigate the full post-buckled behaviour of the structure up to failure.

This paper presents an investigation undertaken by British Aerospace Airbus Ltd into the suitability of nonlinear finite element analysis techniques for the prediction of combined shear and compression post-buckled behaviour of typical wing spar structures.

An experimental test programme was conducted on a full size section of a typical wing spar, with a limited representation of wing skin/stringer structure. The test structure was analysed using the Lawrence Livermore National Laboratory (LLNL) NIKE3D implicit nonlinear finite element code. The analysis included material plasticity and geometric nonlinear effects resulting from combined compression and shear buckling of the spar. In particular the structure's post-buckled behaviour up to failure,

including diagonal tension field stress effects, was investigated.

The analysis was used to predict stresses, strains and displacements during loading, and also to assess the failure mode of the spar specimen. These predicted results were then compared with experimental data obtained from the test programme.

EXPERIMENTAL TEST PROGRAMME

An experimental test programme was conducted on a full sized section of wing spar with a limited representation of wing skin/stringer structure. The object of the test programme was to produce measured test results from a spar under combined shear and compression buckling, including plasticity and diagonal tension field effects.

A cantilever test configuration was chosen to enable combined shear and compression loading to be developed in the top skin and upper portion of the spar. This form of loading was chosen to simulate a spar flight load case.

The test specimen used in this study comprised of five principal components. A section of integrally machined wing spar 4.8 meters in length, top and bottom skin sections 220 mm wide, and test specific top and bottom angle stringers. Some skin reinforcing was used to transfer the end fixation loads smoothly into the test spar and skins, and additional structure was also provided at 'rib' positions to enable lateral support of the test specimen during loading. The basic spar test structure is shown in figure 1.

A NIKE3D nonlinear finite element analysis of the spar test structure was used to identify a target test region on the spar. A total of thirty six strain gauges were applied to the spar panels and skin in the test region. Six displacement transducers were also used to measure the out-of-plane displacements of the spar panels.

Spar, skin and stringer materials were chosen to be representative of an actual wing structure. A material test programme was also conducted to obtain the actual average stress-strain relationship for each component used in the cantilever test structure.
A number of static loading cycles were applied to the test structure until a failure was achieved.

NIKE3D FINITE ELEMENT ANALYSIS

A NIKE3D finite element model of the spar cantilever test specimen was constructed using the LLNL INGRID pre-processor. The finite element model comprised 4257 nodes, 4501 Hughes-Liu shell elements with seven through thickness integration points, and 190 solid elements. The finite element mesh is shown in figure 2.

The model was constructed with the overall aim of concentrating as many elements into the test region as possible whilst limiting the maximum number of elements in the model to remain within practical in-house computer limitations.

The spar geometry was represented as accurately as was practical within the overall modelling limitations. Nominal dimensions were used throughout, apart from the test region, for which measured values were available for both skins and spar panels.

Isotropic elastic-plastic material models were used with the effective stress/effective plastic strain curve input option. Other material property values used were obtained from the material test programme conducted on test components. The load case comprised of a load applied at the tip of the finite element cantilever spar model. The load was applied evenly to the dummy load block in a direction so as to produce tension in the bottom skin and compression in the top skin.

The analysis was performed using the default solution control parameters with bandwidth minimization and the BFGS iteration equilibrium method.

COMPARISON OF EXPERIMENTAL AND ANALYSIS RESULTS

Prediction of Spar Surface Strains

A selection of strain experimental results and their comparison with analysis predictions are presented in figures 3 to 11. Spar or skin strain gauge positions are also indicated in these figures. The analysis results presented are related to element centroidal positions. To enable comparisons with strain locations a number of element results are presented. In each case the element labelled 'A' indicates the element closest to the strain gauge location.

The load point key used in the above figures refer to the experimental results and are as follows:-

points 1 loading to 66%
points 2 loading to 83%
points 3 loading to 100%
points 4 loading to failure

The load percentage values in the above refer to applied analysis loading. This method will be used in this paper for all experimental and finite element load comparisons.

Figures 3, 4 and 5 show the top skin, bottom skin and top spar flange results respectively. Figures 6 to 9 show the upper spar results in the area of the diagonal tension field and secondary bending effects. Figures 10 and 11 show results in the spar's buckled region; this bucking is the result of both shear and compressive loading including plasticity effects.

The above surface strain results show that there is generally reasonable agreement between experiment and analysis prediction.

Prediction of Initial Spar Buckling

The initial spar panel combined shear and compression buckling load was obtained from both panel strain gauge and out-of-plane displacement results. The initial buckling values obtained for the two spar test panels are presented in the following tables:-

Panel 1 Buckling Load

Strain Gauge	42.5%
Displacement Transducer	42.2%
Analysis Prediction	40.0%

Panel 2 Buckling Load

Strain Gauge	45.2%
Displacement Transducer	45.9%
Analysis Prediction	43.6%

The maximum error for prediction of buckle as observed in the above comparison is 6.25%.

The out-of-plane spar panel deflection resulting from the shear/compression buckle is shown in figures 12 and 13 for panels 1 and 2 respectively. These results show that the buckle direction is predicted correctly for each panel. However the maximum error in out-of-plane displacement, corrected for spar movement, was 31.0% and 21.7% for panel 1 and 2 respectively.

Prediction of Plasticity Effects

Two strain gauges have been selected to demonstrate the prediction of plasticity effects. The first gauge, 001 figure 10, is positioned approximately in the middle of panel 1. The second gauge, 016 figure 7, is positioned in the corner of panel 1. Two slope changes in the spar material stress strain curve have been used for comparison purposes. The first is the initial change from linear-elastic properties and the second is the knee in the stress strain curve after which plasticity is fully established. The results below indicate that there is reasonable agreement between experimental and analysis results.

Strain Gauge 001

	Test	Analysis
1st non-linear	56.9%	56.3%
2nd plasticity	80.4%	76.1%

Strain Gauge 016

	Test	Analysis
1st non-linear	59.9%	62.9%
2nd plasticity	84.2%	80.8%

The maximum error for the plasticity prediction as observed in the above comparison is 5.6%

The effects of multiple loading on the spar may be seen in figures 9 and 11. As the test structure is unloaded and reloaded the effects of a build up of permanent panel buckle may be seen. In the NIKE3D analysis no initial panel deformation has been included.

Spar Failure Assessment

The analysis results indicate that the spar panels initially buckle elastically at 40% load. These buckles start to develop plasticity regions on their concave surfaces at about 70% load. The plastic buckled region in panel 1 develops as the load increases and, by 95%, load plastic regions have formed on both sides of the spar.

The maximum shear stress method was used to assess failure in the spar material. Failure was assumed to have taken place when the stresses in the outer fibres of the material had reached this failure condition.

Analysis results predicted failure in panel 1 at 94% load and failure in the upper reinforced area of this panel at 97% load. The experiment failure occurred at 105% load.

These predicted failure values should be considered to indicate a lower bound failure condition. To model fully the spar and skin structure to its ultimate collapse would required a far more detailed simulation including all interfaces and bolt attachments together with a much more refined element mesh. However within the limitations of the finite element model used, a reasonable lower bound failure prediction was obtained.

CONCLUSIONS

Generally reasonable agreement was obtained between analysis and experimental results for predicting the initial buckling load, plasticity effects, surface strains and buckled mode shape. The panel's out-of-plane displacement however was under estimated by up to 31%.

The accuracy of the analysis prediction may be improved by element mesh refinement. However, within the limitation of the finite element model used, reasonable results were obtained. For accurate prediction of ultimate failure, a sufficiently detailed finite element model is required to model fully all likely modes of failure.

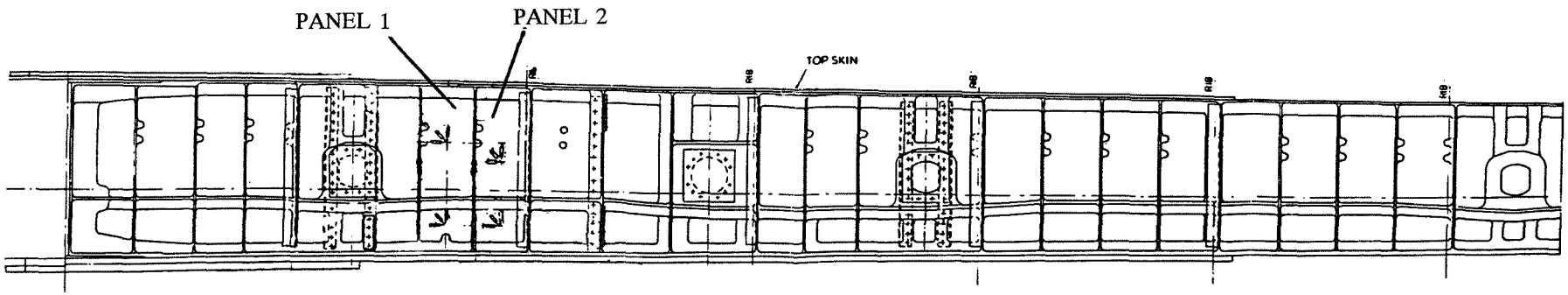

FIGURE 1 SPAR TEST STRUCTURE

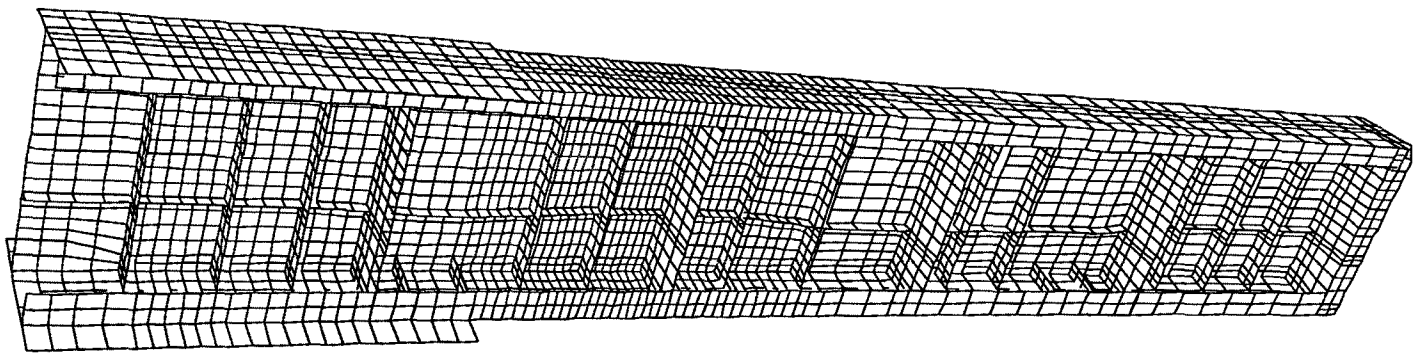

FIGURE 2 FINITE ELEMENT MODEL

FIGURE 3 SPAR TEST STUDY STRAIN GAUGE 033

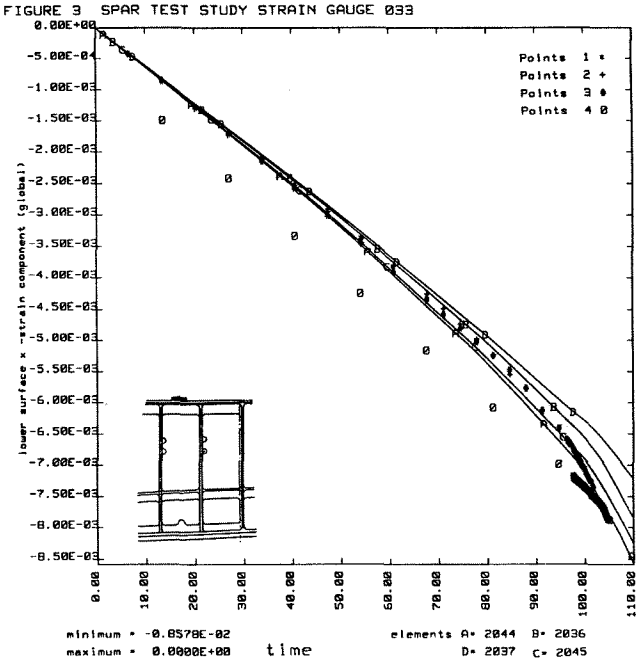

FIGURE 4 SPAR TEST STUDY STRAIN GAUGE 036

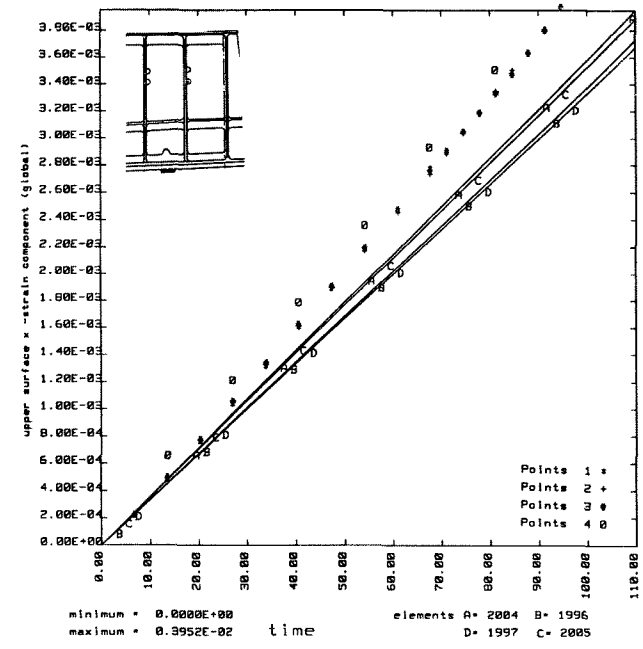

FIGURE 5 SPAR TEST STUDY STRAIN GAUGE 034

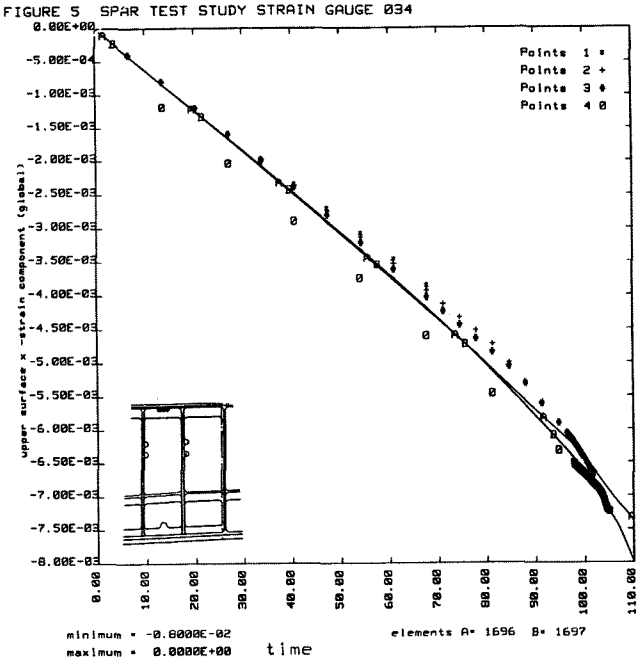

FIGURE 6 SPAR TEST STUDY STRAIN GAUGE 013

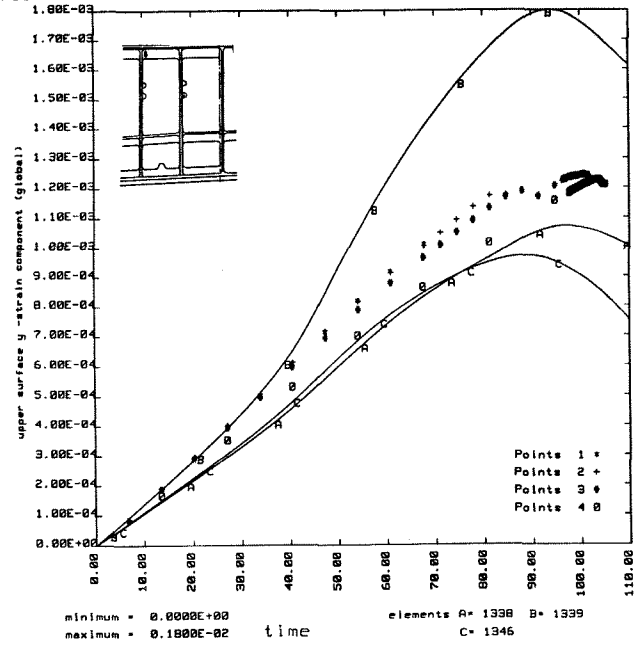

FIGURE 7 SPAR TEST STUDY STRAIN GAUGE 016

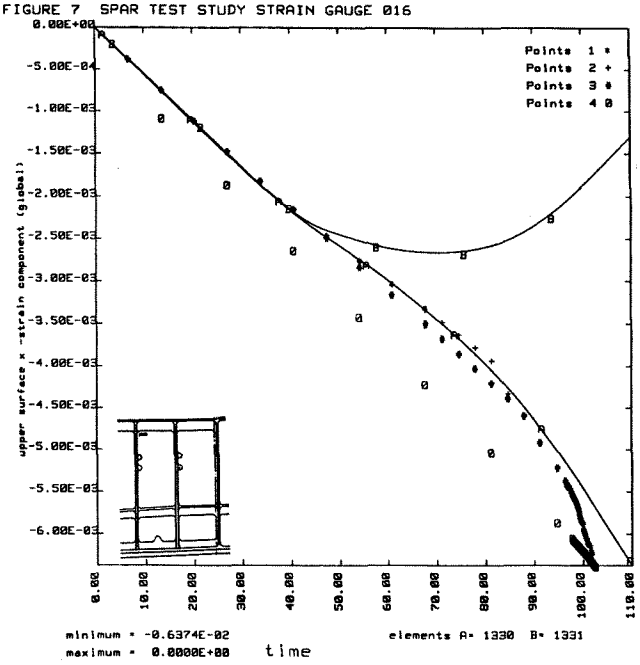

FIGURE 9 SPAR TEST STUDY STRAIN GAUGE 021

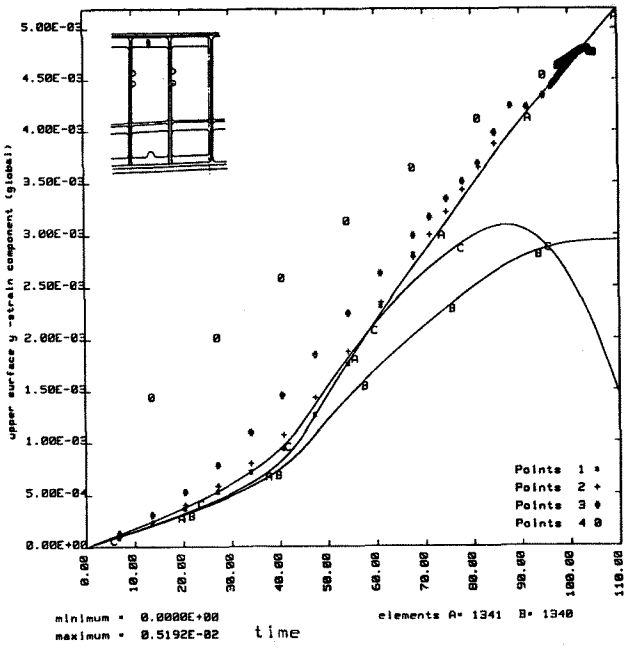

FIGURE 8 SPAR TEST STUDY STRAIN GAUGE 019

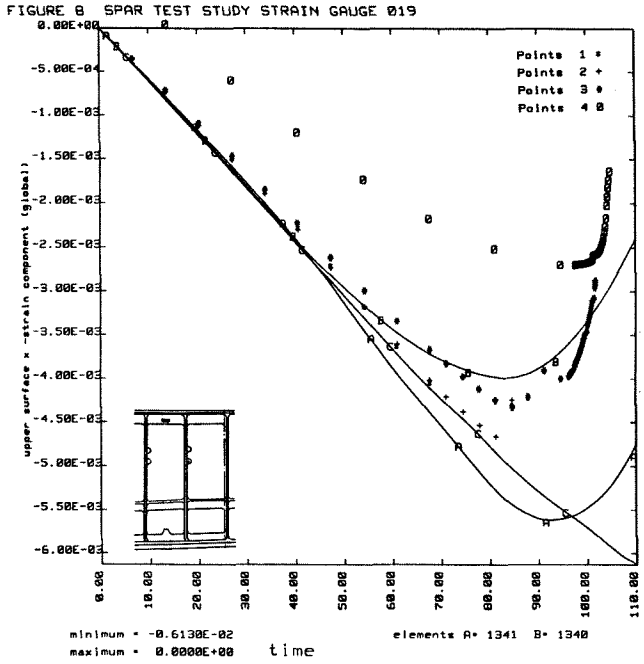

FIGURE 10 SPAR TEST STUDY STRAIN GAUGE 001

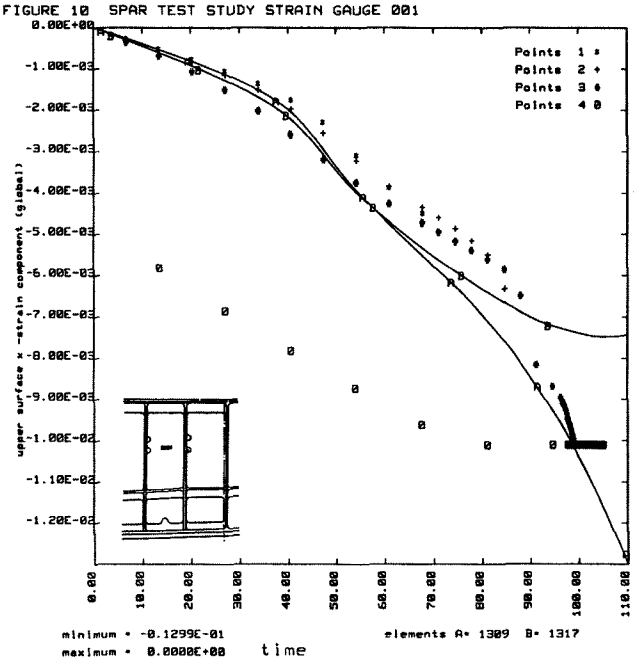

FIGURE 11 SPAR TEST STUDY STRAIN GAUGE 004

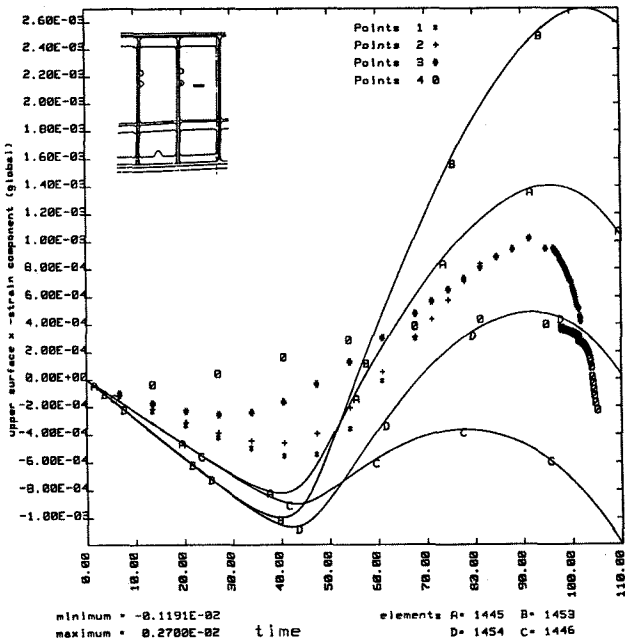

FIGURE 12 PANEL 2 OUT-OF-PLANE DEFLECTION

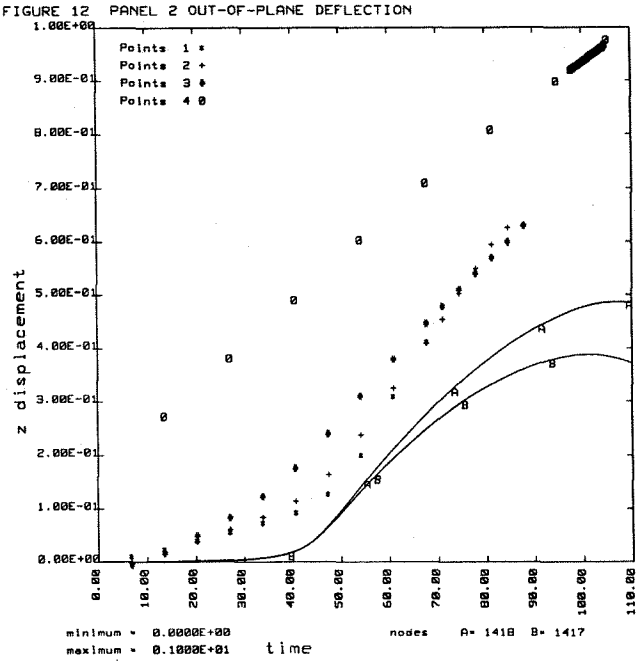

FIGURE 13 PANEL 1 OUT-OF-PLANE DEFLECTION